THE INTERNATIONAL JOURNAL OF SCIENCE & TECHNOLEDGE

Cad Spect/Ct in Managing Liver Tumours and Other Related Abnormalities

Fahad Usman
School of Physics, Universiti Sains, Malaysia, Pulau Penang, Malaysia
Lecturer, Head of Department of Physics, Al-Qalam University Katsina, Tafawa Balewa Way, Katsina, Nigeria
Rafidat Bint Zainon
Senior Lecturer, Oncological and Radiological Sciences Cluster, Advanced Medical and Dental Institute (AMDI) Universiti Sains Malaysia, Kepala Batas, Pulau Pinang, Malaysia
Hayatu Mohammed
Medical Physicist, Department of Radiology, University of Maiduguri Teaching Hospital, Maiduguri, Nigeria
Khairul Jafar Nizam
Technologist, Nuclear Medicine Unit, AMDI, Universiti Sains Malaysia, Pulau Pinang, Malaysia
Mannawi Nasiru Isa
Assistant Lecturer, Department of Physics, Al-Qalam University Katsina, Tafawa Balewa Way, Katsina, Nigeria
Balogun Wasiu Gbolahan
Ph.D. Candidate, Integrative Medicine Cluster, AMDI, Universiti Sains Malaysia, Pulau Pinang, Malaysia

Abstract:
The work evaluates the effect of incorporating OSEM and FBP liver SPECT/CT with a modeled CAD system in managing liver tumors and its relatives. An anthropomorphic torso phantom with lung and liver inserts was injected with ^{99m}Tc. Polystyrene beads filled the lungs inserts. A tumour was mimicked in the liver insert. Sequential SPECT and CT projections were acquired and reconstructed using OSEM and FBP techniques. Segmented and non-segmented SPECT/CT data were modeled and analysed using image j software. Statistical t-test tested the mean grey values of the tumour and its background. The OSEM and FBP reconstructed images were evaluated using contrast to noise ratio (CNR) based on rose criterion. The background and the tumour's mean values were statistically significant. The CNR values for both modeled and non-modeled CAD FBP images were all under the detection range. Nevertheless, its maximum CNR value was at the cutoff frequency 0.48 (1.69). The OSEM reconstructed images displayed peak at 3-4 numbers of iterations. In accession, its modeled CAD evaluation gave CNR values within the detection range from 2-8 numbers of iteration. The non-modeled CAD OSEM reconstructed liver SPECT/CT was below. OSEM was agreed the best in tumour detection and ensuring patient's safety.

Keywords: *Anthropomorphic torso phantom, SPECT/CT, OSEM, FBP, CNR, CAD*

1. Introduction

Primary Liver cancers, including both the Hepatocellular carcinoma (HCC) and the Bile duct cancer (cholangio carcinoma) has been rated among the top cancer types affecting African and Asian regions (Barbosa *et al*., 2015, O'Keefe *et al*., 2015, Hotez *et al*., 2014). Furthermore, the mortality rate resulting from its incidence generally increases. Consequently, the need for a reliable means of detecting the cancers is needed in order to improve the survival rate. Nevertheless, early detection of the cancer is problematic because signs and symptoms of liver cancer tend not to be felt or noticed until the cancer is well advanced (Robinson *et al*., 2014, Sahani *et al*., 2014, Young *et al*., 2014). In gain, proper and accurate sensing of other liver abnormalities assists in the prevention of radiation induced liver disease. This hinders achieving a reasonable survival rate (He *et al*., 2013, Park *et al*., 2014).

Many studies have shown the impact of computed tomography (CT) and magnetic resonance imaging (MRI) in detecting the incidence and the extent of the cancer as well as other abnormalities. The studies were extended to the incorporation of computer aided detection (CAD) with the imaging modalities (Kumar and Devapal, 2014, Dixit and Pruthi, 2014, Wang and Zhang, 2009). Yet, despite all the promising impact of the imaging modalities and CAD systems, a big problem is proper and reliable sensing of the cancers at its early stage (Park *et al*., 2014, He *et al*., 2013, Sherman *et al*., 2012). This trouble is less solved by CT and MRI. This is resulted from their capability of reading just the anatomical information of the cancer, which its manifestation delays. Single photon emission computed tomography (SPECT) detects cancers based on the functional and metabolic processes (Cherry *et al*., 2012, Powsner and Powsner, 2008). Thus, it allows the detection of liver cancer and other related abnormalities at their early stage before any anatomical change. Nonetheless, SPECT suffers an inherent low count leading to its poor resolution (Powsner and Powsner, 2008). Furthermore, it suffers from attenuation, scattering and collimator response effects. Incorporation of SPECT with CT in one

outdoor stage has shown and suggested to increase accuracy in the detection of lesions and abnormalities in the liver (Gates *et al*., 2015, Groheux *et al*., 2013, Shah *et al*., 2015). The CT components play a role of providing both anatomical information as well as an attenuation correction (Ritt *et al*., 2014, Schillaci, 2005, Sharma *et al*., 2013, Patton and Turkington, 2008, Ruf *et al*., 2007). Consequently, an optimal image is obtained. This prevents and manages the occurrence of diseases like radioembolisation induced liver disease (REILD) by depicting the exact extent of the tumour to receive the catheter treatment (Ahmadzadehfar *et al*., 2014, Ahmadzadehfar and Biersack, 2013, Ahmadzadehfar and Hoffmann, 2014, Leal and Wale, 2014). Despite the improvements with SPECT/CT in detecting the lesion, its accurate delineation is unachievable in some cases (Sharma and Kaur, 2013). The problem is more intense among less experienced nuclear medicine physicians and technologists.

This work is aimed at evaluating the modelled CAD system incorporated with the ordered subset expectation maximization (OSEM) and filtered back projection (FBP) reconstructed SPECT/CT image as applied to radioembolisation induced liver disease and other liver abnormalities. The quantitative evaluation uses contrast to noise ratio (CNR) (Charman, 1998, Mettler Jr and Guiberteau, 2011) will be utilised. This is to reduce the difficulties in the medical imaging interpretations among the physicians, especially the less experienced ones.

2. Materials and Methods

2.1. Subject and Data Acquisition Area

The data acquisition was held at the Nuclear Medicine Unit, Clinical Trial Centre, Advanced Medical and Dental Institute, Universiti Sains Malaysia. The unit is installed with dual camera 16 slice Hybrid SPECT/CT system, which was utilised for the image acquisition. The Anthropomorphic Torso phantom with background volume of 10.3 litres contains a liver insert (volume 1.2 litres), lungs insert (0.9 litres and 1.1 litres for left and right respectively) and optional cardiac insert. The acquisition of the SPECT/CT Image was conducted with the cardiac insert not in place. The study concentrated on the Liver insert of the phantom. In the liver insert, a tumour was mimicked using a syringe sphere of about 27 mm diameter, volume of about 30 ml. The diameter of such magnitude was taken so as to prevent the partial volume effect by leaving it to go past the system's spatial resolution which is almost 13 mm FWHM.

2.2. SPECT/CT Acquisition and its Parameters

The SPECT/CT acquisition was performed for 12 minutes. The step and shoot acquisition mode was used following injecting the phantom with ^{99m}Tc. The radioactivity concentrations injected were 0.07 MBq/ml, 0.2 MBq/ml and 2 MBq/ml for the background, liver insert of the phantom and the sphere respectively. Data were acquired using the dual-detector (adjustable) multi-slice (16 slice) CT Scanner (General Electric) equipped with low-energy high-resolution parallel-hole collimators (LEHR). Furthermore, the data were also acquired as 128 × 128 matrices for 120 projections (60 per gamma camera head) at 10 seconds/projection using the 'step and shoot mode'. The tomographic projection views were acquired over an arc of 360º. Energy discrimination was accomplished with a 20% energy window centred on 140 keV. The CT component of the examination was acquired immediately after the SPECT component, without changing the phantom arrangement position. The CT was acquired using a diagnostic setting of 120 kVp at 80 mA and 0.8 s. In addition, the unit was set to acquire 3.75 mm thick slices in spiral acquisition mode. This made the data obtained from the CT acquisition perfect for 3D imaging (because of the lack of motion mis-registration) and the increased out of plane resolution (due to fastest nature associated with it relative to the conventional method of acquisition). The CT data were acquired into 256 × 256 matrices. The CT scan was conducted in 2 minutes; this made the total acquisition time for the SPECT/CT, 12 minutes as mentioned.

2.3. SPECT/CT Image Reconstruction Techniques

The SPECT projections data acquired from the 'step and shoot' acquisition mode were sent to the processing unit of the department. Image processing personal computers (PCs) were situated in the unit. The processing PCs were installed with xyleris software containing FBP and OSEM reconstruction capabilities. The data were reconstructed by both the FBP and OSEM reconstruction algorithms, using different parameter selection. For OSEM reconstruction algorithm, the projection data were reconstructed using 10 numbers of subsets, with 2, 3, 4, 5, 6, 7, 8, 9, and 10 numbers of iterations. The post filtration was made using a Butterworth filter, cut-off frequency 0.48 and order 10 for all the OSEM reconstructed images. Also for the FBP reconstruction, Butterworth filter was used for the noise suppression in a fixed order of 10 and cut off frequencies of 0.38, 0.43, 0.48, 0.53 and 0.58 were used in reconstructing the projection data. Coming after the CT reconstruction, the two images of the different modalities were fused (registered). Furthermore, the OSEM algorithm incorporated corrections for: collimator-specific resolution recovery corrections, scattering corrections, and CT -attenuation corrections.

2.4. Computer Aided Detection (CADe) in Liver SPECT/CT

CADe is defined as a procedure in medicine that assists doctors in the interpretation of medical images in a higher degree of accuracy within a shortest possible time. Imaging techniques in X-ray, MRI, and Ultrasound diagnostics yield a great deal of information, which the radiologist has to analyse and evaluate comprehensively in a short time. CADx systems help scan digital images, *e.g.* from computed tomography, for typical appearances and to highlight conspicuous sections, such as potential diseases. Computer aided detection in liver SPECT/CT imaging is aimed at complementing the effort of interpreting physician toward achieving optimal tumour detection. The difference between computer aided diagnosis (CADx) and computer aided detection (CADe) is that, CADx deals with

tumour characterization while CADe deals with tumour detection (Suzuki, 2012, Doi, 2014, Bogoni *et al*., 2014). The modelled CAD system used in this work comprises of four fundamental components.

2.4.1. Selection of Liver Area

The reconstruction acquired projection data gave rise to the SPECT images. Image processing software built into the processing computers called xeleris performed the following functions:

2.4.1.1. Image Fusion

The reconstructed liver SPECT image was registered to the sequentially acquired CT image. This gave rise to hardware fusion SPECT/CT image. Furthermore; attenuation, scattering and collimator detector response correction were also made. In summation, an important feature of tumour contouring was also accomplished.

2.4.1.2. Exclusion of Other Structures

The xyleris software's function was exploited in excluding all the other structures of the inserts in the phantom other than liver as well as its background.

2.4.2. Segmentation

Segmentation (Partitioning) is the procedure of dividing an image into sections with like attributes such as grey level, colour, grain, luminosity, and contrast. The goal of the process is to simplify and/or change the representation of an image into something that is more meaningful and easier. Segmentation process can be achieved by thresholding, edge based detection or region based segmentation. However, thresholding suffers activity inhomogeneity and artefact problems. Consequently, in this work we used edge based detection algorithm available on Image J software called find edge menu. The find edges used a Sobel edge detector to highlight sharp changes in intensity in the selection. Two 3x3 convolution kernels (shown below) were applied to generate vertical and horizontal derivatives. The final image was produced by combining the two derivatives using the square root of the sum of the squares. Ultimately, tumour and background area were clearly differentiated.

2.4.3. Volume of Interest Selection

Following the segmentation process, a clear extent of the tumour was delineated. Thus, a fit eclipses selection menu was used for the proper marking of the volume of interest. Ultimately, the values depicting the quality of the image were measured and evaluated.

2.4.4. Image J Software in Statistical Analysis and Statistical test for SPECT/CT in CAD and non-CAD System

The analysis of the SPECT/CT was also conducted using the open source image processing software (Image J). It is a software based on Java, which was developed at the National Institute of Health, Bethesda, Maryland, USA. Because of its open nature, accessibility to it became easy. However, image processing personal computers give the reconstructed SPECT/CT images' information in DICOM format. This prevented it from losing any of its property. Furthermore, in the process of the analysis, the following basic steps were followed during the analysis:

- The first step was opening the Image J software. This led to the appearance of the tool box with the following labels: File, Edit, Image, Processing, analyse, Plugins, Window and Help.
- Click on File ⟶ Open ⟶ image was selected from the Computer file.
- Click on Edit ⟶ this was to confirm that the image was in DICOM format
- Click on process Find Edges was selected, it uses a Sobel edge detector to highlight sharp changes in intensity in the active image or extract. This helped accurately tracing tumour edges (a segmentation process).
- Click on Image ⟶ Type ⟶ select 8-bit ⟶ the tumour volume was marked.
- Click on image ⟶ properties ⟶ Set scale ⟶ set measurements
- Click analyse ⟶ set measurement ⟶ measure
- Then the result page will appear. From the result page the following measurements were obtained: Mean value, Maximum and Minimum grey value and Standard deviation of the selection among others.
- The same procedure was repeated for another volume of the same magnitude with the background, which was selected in the background region immediately close to the tumour, the same statistical measurements were also obtained.
- The third batch of the analysis was conducted in similar manner as above. However, the evaluation was done at the exclusion of the segmentation.

The t-test (also sometimes called the Student t-test) was then used to determine the significance of the difference between the means of the background and tumour for both the segmented and non-segmented images. This test was aimed at comparing their differences in means relative to the observed random variations in tumour and the background. The significance level of 0.05 levels was set, therefore for all the tests, probability (p) values < 0.05 were considered statistically significant and the null hypothesis was rejected. The statistical test was conducted Microsoft excel 2007 version, using Independent data and one-sided test selection (one tail distribution). All the data were ensured statistically significant before the image quality evaluation was commenced.

2.5. Evaluation of Image Quality in SPECT/CT and its Parameters

Following the statistical calculations and the statistical tests, SPECT/CT Image quality was evaluated. Because of the tomographic reconstruction process in SPECT/CT image, its noise is no longer Poissonian. In addition, it does not have a uniform (white) power spectrum. Furthermore, it depends on a number of parameters: counts acquired in the distribution of the counts, the reconstruction process among the others. Consequently, the raw signal-to-noise ratio is not well behaved and therefore, we used a measure of tomographic contrast, or tomographic contrast-to-noise ratio, in assessing the detectability of the SPECT/CT image. It was calculated using the following formulas. However, the two components of the formula, Contrast and coefficient of variation (which describes the noise) were evaluated first.

Contrast: This refers to the differences in density (or intensity) in parts of the image. It was evaluated using the following relation:

Contrast (C) $= \frac{\bar{S} - \bar{b}}{\bar{b}}$ (Cherry *et al*., 2012)

Where, $\bar{S}$ is the mean value of the high concentration VOI (tumour) and $\bar{b}$ is the mean value of the background VOI.

Noise (represented by the background standard deviation): This can be described as an undesirable by-product of image capture that adds spurious and extraneous information. Statistical noise can impair detectability, especially if the object has low contrast. The coefficient of variation (N), also known as "relative variability", which was applied in calculating the CNR, equals the standard deviation divided by the mean. It was expressed as a fraction.

$\mathbf{N} = \frac{\boldsymbol{\sigma b}}{\bar{\mathbf{b}}}$ (Cherry *et al*., 2012)

Following the components' evaluation, the essential parameter for evaluating detectability, the CNR (contrast to noise ratio) of the object in the image was then evaluated. The conclusion was reached that, for detectability to be achieved, an object's CNR must exceed 3-5 (Cherry et al., 2012). This condition is known as the Rose criterion.

Contrast to Noise Ratio (CNR) = $\frac{C}{N}$ (Cherry *et al*., 2012) Where, N is the noise contrast (coefficient of variation), $\boldsymbol{\sigma_b}$ is the Standard deviation of the liver insert background, $\bar{\mathbf{b}}$ is the mean intensity of the background counts, $\bar{S}$ is the mean value of the high concentration VOI (tumour) and C is its contrast.

3. Results

Cut- off frequency	CNR
0.38	1.39
0.43	1.42
0.48	1.69
0.53	1.37
0.58	1.36

Table 1: CNR for CAD FBP reconstructed SPECT/CT (step and shoot acquisition) using 10 subsets versus cut off frequencies

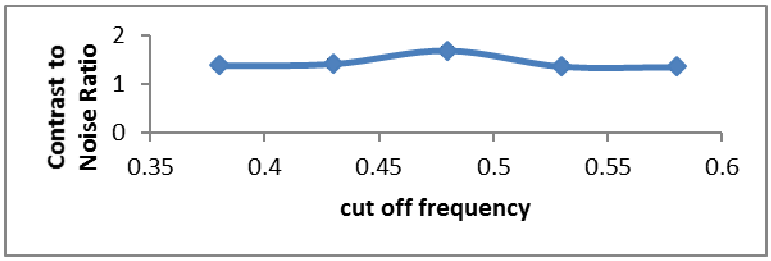

Figure 1: CNR for CAD FBP reconstructed SPECT/CT (step and shoot acquisition) using 10 subsets versus cut off frequencies

Iterations	CNR
2	3.71
3	3.84
4	3.89
5	3.67
6	3.58
7	3.38
8	3.17
9	2.57
10	2.01

Table 2: CNR for CAD OSEM reconstructed SPECT/CT (step and shoot acquisition), 10 subsets versus Numbers of iterations

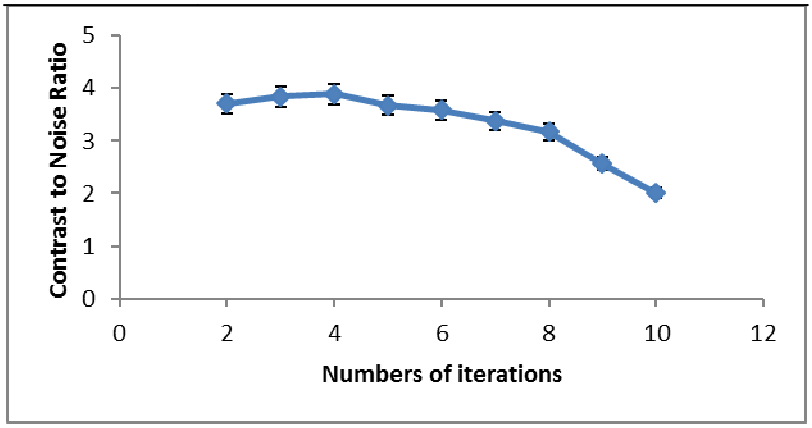

Figure 2: CNR for CAD OSEM reconstructed SPECT/CT (step and shoot acquisition), 10 subsets versus Numbers of iterations

Cut- off frequency	CNR
0.38	1.27
0.43	1.54
0.48	1.68
0.53	1.57
0.58	1.57

Table 3: CNR for CAD FBP reconstructed SPECT/CT (step and shoot acquisition) using 10 subsets versus cut off frequencies

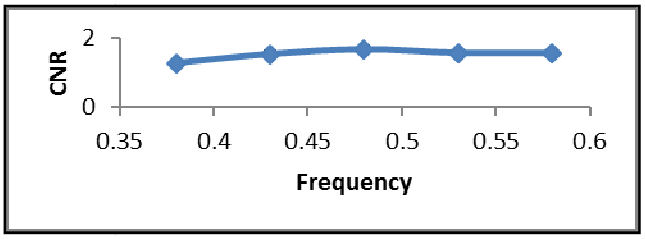

Figure 3: CNR for FBP reconstructed SPECT/CT (step and shoot acquisition) using 10 subsets versus cut-off frequencies

Iterations	CNR
2	1.68
3	2.27
4	2.04
5	1.57
6	1.51
7	1.47
8	1.47
9	1.39
10	1.38

Table 4: CNR for OSEM reconstructed SPECT/CT (step and shoot acquisition), 10 subsets versus Numbers of iterations

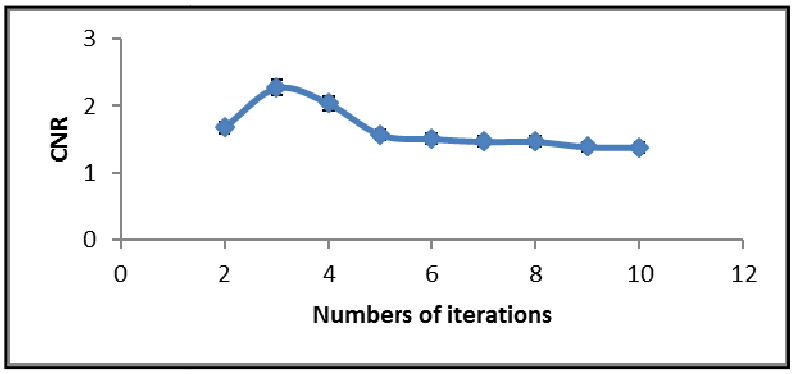

Figure 4: CNR for CAD OSEM reconstructed SPECT/CT (step and shoot acquisition), 10 subsets versus Numbers of iterations

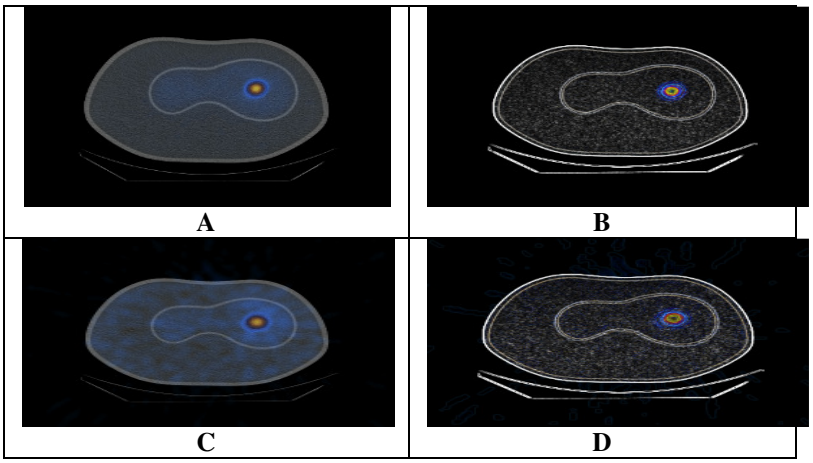

Figure 5: (A) Non-segmented OSEM reconstructed liver tumour SPECT (B) Segmented OSEM reconstructed liver tumour SPECT (C) Non- segmented FBP liver tumour SPECT (D) Segmented FBP liver tumour SPECT

SPECT/CT images showed different, but interesting result. The SPECT/CT image quality varies as a consequence of different parameter selection as well as the computing system used in aiding the tumour detection. Established on the types of the reconstruction techniques, FBP reconstructed SPECT/CT showed a less magnitude in terms of the signal and relatively high level of the statistical noise. Its CNR values for all its selected parameters falls below the detection limit set by rose criterion. These include both the computer aided and non-computer aided SPECT/CT images (Figure 1 and Figure 3). However, FBP reconstructed SPECT/CT that incorporates Computer aiding system showed an improvement in the magnitude of the CNR compared to the non-aided one (Table 1). Furthermore, both the aided and non-aided showed a similar pattern. The CNR value rises initially until it reached a peak at the cut-off frequency 0.48 (Figure 1 and Figure 3). The CNR value, then decreases with increasing cut-off frequency.

The quality of SPECT/CT image reconstructed by OSEM algorithm showed an interesting solution. The results showed that, both the aided and non-aided have a similar pattern (peak at about three to four numbers of iterations) (Figure 2 and Figure 4). Nonetheless, the attracting difference is in the range of lesion detection described by the rose criterion (CNR=3-5). The aided OSEM reconstructed SPECT/CT have its CNR values within the range of detection from 2-8 numbers of iterations (Figure 2). But, alas for the non-aided one, the CNR values in all the numbers of iteration are below the range of detectability (Figure 4). This makes the importance of using Computer aided detection apparent. Consequently, tumour detection is achieved with greater accuracy due to the proper segmentation of the liver SPECT/CT image as shown (Figure 2). The tumour boundary is easily recognized following the utilization of the different intensity representation in the liver tumour and background (Figure 5). The variation in the intensity eased the proper marking of the actual extent of the tumour from the overall image. In addition, the achievement was attained at a limited time. Consequently, the examination period reduction added value to CAD incorporated SPECT/CT image. All these were nowhere to be found in case of non-computer aided liver SPECT/CT image. Ultimately, the result of the liver SPECT/CT image showed the OSEM reconstruction method to be superior to FBP in terms of liver tumour detection (Figure 2 and Figure 4). In addition, the result easily deduced that the effect of Computer aided detection on ordered subset expectation maximization (OSEM) is greater compared to Filtered back projection (FBP) reconstructed images. Furthermore, the issue of boundary is achieved from the incorporated CT in the image.

4. Discussion

SPECT or Planer acquisitions cannot determine the situation of a tumour for better characterization with accuracy (Aparici *et al*., 2011, Keidar *et al*., 2003, Lavely *et al*., 2007). The diligence of novel engineering science that combines functional and anatomic information, the SPECT/CT images has proven to improve the detection of liver tumours and other liver abnormalities (Kim, 2014, Mariani *et al*., 2010). Sometimes, accumulation of 99^{m}Tc on the liver surface could be accepted for either planer or SPECT imaging, especially in the case of single tumours. However, only SPECT/CT can detect with greater precision the distribution of the radionuclide in many complicated cases like multiple tumours, metastases, low contrast functional imaging among the others (Mariani *et al*., 2010). This results from the low spatial resolution, significant partial volume effect and statistical nature of the radioactive decay that are linked with nuclear medicine imaging in general.

The computer aid detection system has been shown to assist radiologists and other medical imaging interpreters toward achieving greater accuracy compared to the radiologists alone (Kumar and Devapal, 2014). In the case of liver abnormalities, many studies showed how computer aided detection system improve the quality of medical imaging. However, most of the studies on the liver CAD focus on computed tomography (CT) and magnetic resonance imaging (MRI). Several CAD systems for detection and diagnosis were developed by different researchers. Furthermore, these systems all showed an improvement in terms of confidence increment as well as minimization of the reading time.

In the present study, nuclear medicine imaging (SPECT) was used for the evaluation of the modeled CAD system in detecting liver tumour. This is imputable to its capability of detecting abnormality before any anatomical manifestations (Powsner and Powsner, 2008, Fanti *et al*., 2011, Groch and Erwin, 2000). The CT image acquisition that was carried out sequentially with the SPECT using the same bed setting gave many advantages. These include: attenuation correction, contouring of the tumour boundary among others. The study showed a similar result regarding improvement in the interpretation of tumours on liver medical imaging obtained from CT

and MRI. The graph pattern showed by FBP reconstructed liver SPECT/CT implies how contrast and noise trade-off is being reached (Figure 1 and Figure 3). Initially, the noisy liver SPECT was smoothed after applying the Butterworth filter of 0.38 cut off frequencies to it. This initial application of the filter seriously affected the contrast of the picture. As a result the Contrast to Noise Ratio (CNR) is less. Only, as we increased cut-off frequency, the contrast and the spatial resolution improve a little number at the expense of increased interference. However, despite the noise increment and the contrast reduction, the pattern of the graph before the peak implied the dominance of contrast over the noise up to the peak (Figure 1 and Figure 3). But, at greater cut-off frequencies of 0.53 and above, the noise contribution became greater than the one observed before the peak. Consequently, CNR value decreases after 0.48 cut-off frequencies and above.

In the case of OSEM reconstructed SPECT images (Figure 2 and Figure 4), the higher frequency noise signals were constantly suppressed by the fixed application of Butterworth filter of 0.48 cut-off frequencies. Nevertheless, the similarity of its graph pattern with that of FBP reconstructed images is explained from a dissimilar view. Granting to the surveys conducted by many researchers, increasing the iteration number takes the images closer to the real image. Consequently, spatial resolution and the image contrast increases. Thus, CNR increases with increasing numbers of iterations up to the peak at about 4 numbers of iterations. After the peak it decreases progressively. This resulted from the fact that, at small numbers of iterations, the increase in high frequency noise is less (Cherry *et al*., 2012). Furthermore, the low pass filter (Butterworth) suppressed all the characteristic noisy signals at higher frequencies than its cut-off frequency. Hence, we can also conclude that the trade-off between contrast and noise ratio is also the main determiner. As the numbers of iterations were increased, noise and contrast increases as well. However, before reaching the peak at about 4 numbers of iterations, the contrast is greater than the noise build-up (Koch *et al*., 2005, McConnell *et al*., 2012, Nichols *et al*., 2015). Furthermore, after passing the peak, the noise builds up seems to be dominated relative to the contrast. Consequently, CNR value decreases progressively.

The detection ability based on the limit set by Rose criterion showed that non-computer aided SPECT/CT is not capable of proper detection (Figure 1 and Figure 2). This is resulted from its failure to reach the CNR value of at least 3.

Therefore, we suggest that CAD system incorporated with SPECT/CT be used in order to achieve a reasonable detection limit. Furthermore, OSEM is the reconstruction algorithm to be constantly used for proper tumour detection. In addition, quantitative evaluation should be used for validating the qualitative evaluation method. This is because; qualitative method is characterized by subjectivity. Ultimately, proper interpretation became less reliable, especially in the case of inexperience or less experience radiologist or any other interpreting personnel.

5. Conclusion

CAD in Liver SPECT/CT image achieves its goals by utilizing an OSEM reconstruction algorithm. It is also shown that, qualitative evaluation can be successfully replaced by quantitative one. This would be beneficial to less experience interpreting personnel. Furthermore, in OSEM reconstruction, at around four (4) numbers of iterations, the administered activity of the radionuclide can be brought down. Therefore, the patient and the personnel exposure to radiation would be cut. In addition, above all, incorporating the CAD system in SPECT can prevent any complication in liver SPECT imaging. This is because of its ability to detect the functional and metabolic processes in the liver that normally appears long ago before any anatomical manifestations. In summation, a well-developed CAD system in liver SPECT/CT and other functional and molecular images should be focused by researchers. This would be of great help in the management of almost all the liver related abnormalities at their earliest stage.

6. Acknowledgement

The authors will like to appreciate the role of the entire staff of nuclear medicine unit, AMDI and School of Physics, all at the Universiti Sains Malaysia (USM) for their invaluable assistance in this work. In addition, the tireless effort by the management of Al-Qalam University, Particularly, the Vice Chancellor, Prof. Shehu Ado Garki is highly appreciated

7. References

i. Ahmadzadehfar, H. & Biersack, H.-J. 2013. Clinical applications of SPECT-CT, Springer Science & Business Media, 61-85
ii. Ahmadzadehfar, H., Duan, H., Haug, A. R., Walrand, S. & Hoffmann, M. 2014. The role of SPECT/CT in radioembolization of liver tumours. European journal of nuclear medicine and molecular imaging, 41**,** 115-124.
iii. Ahmadzadehfar, H. & Hoffmann, M. 2014. Therapy Planning with SPECT/CT in Radioembolisation of Liver Tumours. Clinical Applications of SPECT-CT. Springer, 255-270
iv. Aparici, C. M., Avram, A. M., Castrejón, A. S., Dvorak, R. A., Erba, P., Fettich, J., Garcia, J. M. C., García, V. M. P., Hawkins, R. & Hodolic, M. 2011. SPECT-CT for Tumor Imaging. Atlas of SPECT-CT. Springer, 15-104
v. Barbosa, I. R., De souza, D. L., Bernal, M. M. & Do CC Costa, Í. 2015. Cancer mortality in Brazil: Temporal Trends and Predictions for the Year 2030. Medicine, 94**,** e746.
vi. Bogoni, L., Cathier, P., Dundar, M., Jerebko, A., Lakare, S., Liang, J., Periaswamy, S., Baker, M. & Macari, M. 2014. Computer-aided detection (CAD) for CT colonography: a tool to address a growing need. The British Journal of Radiology, 78,57-62
vii. Charman, W. 1998. Imaging in the 21st century. Ophthalmic and Physiological Optics, 18**,** 210-223.
viii. Cherry, S. R., Sorenson, J. A. & Phelps, M. E. 2012. Physics in nuclear medicine, Elsevier Health Sciences.1-223
ix. Dixit, V. & Pruthi, J. 2014. Review of Image Processing Techniques for Automatic Detection of Tumor in Human Liver, International Journal of Computer Science and Mobile Computing, 3,371-378

x. Doi, K. 2014. Current status and future potential of computer-aided diagnosis in medical imaging. The British Journal of Radiology, 68, 79-93

xi. Fanti, S., Farsad, M. & Mansi, L. 2011. Atlas of SPECT-CT, Springer Science & Business Media.pp 1-255

xii. Gates, V. L., Singh, N., Lewandowski, R. J., Spies, S. & Salem, R. 2015. Intraarterial Hepatic SPECT/CT Imaging Using 99mTc-Macroaggregated Albumin in Preparation for Radioembolization. Journal of Nuclear Medicine, 56**,** 1157-1162.

xiii. Groch, M. W. & Erwin, W. D. 2000. SPECT in the year 2000: basic principles. Journal of Nuclear Medicine Technology, 28**,** 233-244.

xiv. Groheux, D., Giacchetti, S., Delord, M., Hindié, E., Vercellino, L., Cuvier, C., Toubert, M.-E., Merlet, P., Hennequin, C. & Espié, M. 2013. 18F-FDG PET/CT in staging patients with locally advanced or inflammatory breast cancer: comparison to conventional staging. Journal of Nuclear Medicine, 54**,** 5-11.

xv. He, G., Dhar, D., Nakagawa, H., Font-burgada, J., Ogata, H., Jiang, Y., Shalapour, S., Seki, E., Yost, S. E. & Jepsen, K. 2013. Identification of liver cancer progenitors whose malignant progression depends on autocrine IL-6 signaling. Cell, 155**,** 384-396.

xvi. Hotez, P. J., Alvarado, M., Basáñez, M.-G., Bolliger, I., Bourne, R., Boussinesq, M., Brooker, S. J., Brown, A. S., Buckle, G. & Budke, C. M. 2014. The global burden of disease study 2010: interpretation and implications for the neglected tropical diseases.8,7

xvii. Keidar, Z., Israel, O. & Krausz, Y. 2003. SPECT/CT in tumor imaging: technical aspects and clinical applications. Seminars in nuclear medicine, Elsevier, 205-218.

xviii. Kim, E. E. 2014. Clinical Applications of SPECT-CT. Journal of Nuclear Medicine, 55**,** 2078-2080.

xix. Koch, W., Hamann, C., Welsch, J., Pöpperl, G., Radau, P. E. & Tatsch, K. 2005. Is iterative reconstruction an alternative to filtered backprojection in routine processing of dopamine transporter SPECT studies? Journal of Nuclear Medicine, 46**,** 1804-1811.

xx. Kumar, S. S. & Devapal, D. 2014. Survey on recent CAD system for liver disease diagnosis. Control, Instrumentation, Communication and Computational Technologies (ICCICCT), 2014 International Conference, IEEE, 763-766.

xxi. Lavely, W. C., Goetze, S., Friedman, K. P., Leal, J. P., Zhang, Z., Garret-mayer, E., Dackiw, A. P., Tufano, R. P., Zeiger, M. A. & Ziessman, H. A. 2007. Comparison of SPECT/CT, SPECT, and planar imaging with single-and dual-phase 99mTc-sestamibi parathyroid scintigraphy. Journal of Nuclear Medicine, 48**,** 1084-1089.

xxii. Leal, J., Rowe, S. & Wahl, R. 2014. Performance comparison of Auto-PERCIST (a semi-automated PERCIST-based CAD system) and a clinician in the measurement of PERCIST 1.0 metrics for response assessment. Journal of Nuclear Medicine, 55**,** 2073-2076.

xxiii. Mariani, G., Bruselli, L., Kuwert, T., Kim, E. E., Flotats, A., Israel, O., Dondi, M. & Watanabe, N. 2010. A review on the clinical uses of SPECT/CT. European journal of nuclear medicine and molecular imaging, 37**,** 1959-1985.

xxiv. McConnell, D., Kemp, B., Hunt, C., Johnson, G. & Lowe, V. 2012. Evaluation of an iterative reconstruction algorithm that models the detector response of the PET scanner. Journal of Nuclear Medicine, 53**,** 2618.

xxv. Mettler JR, F. A. & Guiberteau, M. J. 2011. Essentials of nuclear medicine imaging, Elsevier Health Sciences.1-130

xxvi. Nichols, K. J., Tronco, G. G. & Palestro, C. J. 2015. Effect of reconstruction algorithms on the accuracy of 99mTc sestamibi SPECT/CT parathyroid imaging. American journal of nuclear medicine and molecular imaging, 5**,** 195.

xxvii. O'keefe, E. L., Dinicolantonio, J. J., Patil, H., Helzberg, J. H. & Lavie, C. J. 2015. Lifestyle Choices Fuel Epidemics of Diabetes and Cardiovascular Disease among Asian Indians. Progress in cardiovascular diseases. Volume 58, Issue 5, 505–513

xxviii. Park, G., Kim, Y., Kim, C., Yu, H. & Hwang, S. 2014. Diagnostic efficacy of gadoxetic acid-enhanced MRI in the detection of hepatocellular carcinomas: comparison with gadopentetate dimeglumine. The British journal of radiology, 83:996, 1010-1016

xxix. Patton, J. A. & Turkington, T. G. 2008. SPECT/CT physical principles and attenuation correction. Journal of nuclear medicine technology, 36**,** 1-10.

xxx. Powsner, R. A. & Powsner, E. R. 2008. Essential nuclear medicine physics, John Wiley & Sons. 1-113

xxxi. Ritt, P., Sanders, J. & Kuwert, T. 2014. SPECT/CT technology. Clinical and Translational Imaging, 2**,** 445-457.

xxxii. Robinson, P., Arnold, P. & Wilson, D. 2014. Small "indeterminate" lesions on CT of the liver: a follow-up study of stability. The British journal of radiology,76:912, 866-874

xxxiii. Ruf, J., Seehofer, D., Denecke, T., Stelter, L., Rayes, N., Felix, R. & Amthauer, H. 2007. Impact of image fusion and attenuation correction by SPECT-CT on the scintigraphic detection of parathyroid adenomas. Nuklearmedizin, 46**,** 15-21.

xxxiv. Sahani, D. V., Bajwa, M. A., Andrabi, Y., Bajpai, S. & Cusack, J. C. 2014. Current status of imaging and emerging techniques to evaluate liver metastases from colorectal carcinoma. Annals of surgery, 259**,** 861-872.

xxxv. Schillaci, O. 2005. Hybrid SPECT/CT: a new era for SPECT imaging? European journal of nuclear medicine and molecular imaging, 32**,** 521-524.

xxxvi. Shah, K., Gendel, V., Becker, M. & Kempf, J. 2015. 99m Technetium-Macroaggregated Albumin (MAA) SPECT/CT Liver Perfusion Imaging Prior to Radioembolization: Patterns and Pitfalls of Extrahepatic Activity. Journal of Nuclear Medicine, 56**,** 1876.

xxxvii. Sharma, A. & Kaur, P. 2013. Review of CAD Techniques for Liver Tumor Detection. International Journal of Advanced Research in Computer Science and Software Engineering, 3.

xxxviii. Sharma, P., Dhull, V. S., Jeph, S., Reddy, R. M., Singh, H., Naswa, N., Bal, C. & Kumar, R. 2013. Can hybrid SPECT-CT overcome the limitations associated with poor imaging properties of 131I-MIBG?: comparison with planar scintigraphy and SPECT in pheochromocytoma. Clinical nuclear medicine, 38**,** e346-e353.

xxxix. Sherman, M., Bruix, J., Porayko, M. & Tran, T. 2012. Screening for hepatocellular carcinoma: the rationale for the American Association for the Study of Liver Diseases recommendations. Hepatology, 56**,** 793-796.

xl. Suzuki, K. 2012. A review of computer-aided diagnosis in thoracic and colonic imaging. Quantitative imaging in medicine and surgery, 2**,** 163.

xli. Wang, J. X. & Zhang, T. T. 2009, CT Image Segmentation by using a FHNN Algorithm Based on Genetic Approach. Bioinformatics and Biomedical Engineering, 2009. ICBBE 2009. 3rd International Conference. IEEE, 1-4.

xlii. Young, P. E., Womeldorph, C. M., Johnson, E. K., Maykel, J. A., Brucher, B., Stojadinovic, A., Avital, I., Nissan, A. & Steele, S. R. 2014. Early detection of colorectal cancer recurrence in patients undergoing surgery with curative intent: current status and challenges. Journal of Cancer, 5**,** 262.